



OPEN *In vitro* release kinetics and *in vivo* plasma exposure of green tea polyphenols and caffeine from iron oxide chitosan nanoparticles

Safaa Al Awawdeh¹, Nurul Husna Shafie^{1,2}✉, Amirah Haziyah Ishak¹, Norhaizan Mohd Esa^{1,2}, Su Peng Loh¹ & Armania Nurdin^{2,3}

Green tea polyphenols (GTPP) are known for their antioxidant and anticancer activities but suffer from low bioavailability due to instability in the gastrointestinal environment. This study aimed to enhance the oral delivery of GTPP by encapsulating epicatechin, epigallocatechin gallate (EGCG), catechin, gallic acid, theaflavin, and caffeine into iron oxide chitosan nanoparticles (IOCHNP). Using high performance liquid chromatography (HPLC), the release of GTPP was evaluated *in vitro* and *in vivo* in both simulated intestinal media and rat's plasma. GTPP-IOCHNP efficiently encapsulates GTPP, achieving an encapsulation efficiency of 90.9% for catechin and 83.3% for theaflavin. Additionally, less than 8% of GTPP is released in simulated gastric fluid (SGF), while its more readily released in simulated intestinal fluid (SIF) is enhanced, reaching 70% for caffeine. The release of gallic acid and epicatechin followed Higuchi kinetics, catechin followed Korsmeyer-Peppas, and caffeine followed Weibull model, indicating diverse mechanisms of release. The *in vivo* results demonstrated that GTPP loaded GTPP-IOCHNP significantly enhanced the absorption of GTPP compared to GTPP administered alone ($p < 0.05$). The bioavailability of EGCG, epicatechin, catechin, gallic acid and theaflavin was improved by approximately 8.5-, 6.5-, 4.8-, 5- and 3.5- fold respectively when delivered using GTPP-IOCHNP as a carrier. These findings highlight the potential of IOCHNP as an efficient oral delivery platform for tea polyphenols.

Keywords *In vitro*, *In vivo*, Iron oxide, Chitosan, Nanoparticle, Polyphenols

Tea polyphenols represent a broad class of compounds, including approximately 30 distinct phenolic types, with catechins accounting for 30–42% of total polyphenol content¹. Epicatechin, epigallocatechin, epicatechin gallate and epigallocatechin gallate EGCG are main catechin found in green tea. EGCG, in particular, the most potent antioxidant tea catechins and has garnered considerable research attention because of its potential health benefits². In addition to catechins, other important GTPP components include flavonols (5–10%) and other flavonoids³, as well as gallic acid, theaflavins, and caffeine. These compounds have demonstrated various bioactivities: including anticancer, anti-inflammatory and cardioprotective properties⁴.

However, GTPP are extremely unstable and consider as reactive substances, due to their chemical structures, subsequences and high vulnerability to physical, chemical and biological stressors throughout during food processing, distribution, storage, ingestion and digestion⁵. Different impacts on the bioactivities and bioavailability of tea polyphenols result from their unique biotransformation in their microbial, hepatic and intestinal metabolism⁶. As a result, the pharmacokinetic restrictions diminish their targeting efficacy and total therapeutic potential when administered orally⁷. Studies specify that, after the oral administration of an EGCG in rats, approximately, 5% of EGCG is absorbed into systemic circulation⁸. The low oral absorption following oral administration of GTPP mainly because of weak intestinal permeability and poor stability within the gastrointestinal tract. Recently elucidated that 80% of EGCG breaks down in simulated intestinal medium at pH 7.4 (37 °C) 1 h period⁹. Additionally, *in vitro* studies utilizing colorectal adenocarcinoma cells (Caco-2) have been conducted to test the transepithelial transport of gallic acid molecules across the cellular barrier.

¹Department of Nutrition, Faculty of Medicine and Health Sciences, Universiti Putra Malaysia, Serdang 43400, Selangor, Malaysia. ²Laboratory of UPM-MAKNA Cancer Research, Institute of Bioscience, Universiti Putra Malaysia, Serdang 43400, Selangor, Malaysia. ³Department of Biomedical Sciences, Faculty of Medicine and Health Sciences, Universiti Putra Malaysia, Serdang 43400, Selangor, Malaysia. ✉email: nhusnashafie@upm.edu.my

Under a proton gradient, the apparent permeability coefficient was found to be approximately 0.20×10^{-6} cm/s, indicating a notably low permeability level¹⁰. Hence, to achieve the maximum therapeutic benefits of these green tea polyphenols, the oral absorption of GTPP needs to be improved.

There is yet great anticipation in the research areas of the bioavailability of tea polyphenols. A range of strategies has been employed to enhance the limited bioavailability and cellular uptake of GTPP, including the application of nanotechnology and encapsulation techniques¹¹. Nano delivery systems for GTPP are becoming increasingly popular due to their potential advantages in enhancing the bioavailability, stability and targeted delivery of these compounds¹².

Numerous studies have investigated the enhancement of polyphenol bioavailability using various nanoparticle-based delivery systems. Specifically, gelatin nanoparticles¹³, polymeric micelles¹⁴, nanoliposomes¹⁵, nanogels¹⁶ and dendrimers¹⁷ have been developed and evaluated for their potential to improve the bioavailability of these polyphenols compounds. However, even though these organic systems, they provide superior structural stability, but the concerns are regarding cytotoxicity and disruption of cellular membranes persist¹⁸. Therefore, magnetic iron oxide nanoparticles (IONP) are the most widely used magnetic nanoparticles because of their favorable magnetic properties, superior biocompatibility and low cost. They have been extensively studied in many domains, such as environmental science, biomedicine, sensing, energy storage, and electronic devices. IONP are usually considered biocompatible and extensively employed in biomedical applications¹⁹. Furthermore, magnetic nanoparticles possess unique characteristics, such as the ease of modification of their surface chemistry to achieve better compatibility and selectivity. Green tea catechins and iron oxide-based nanoparticles have demonstrated promise in a range of biomedical applications, such as cancer treatment and drug delivery. These nanoparticles have been shown to have better cellular absorption, bioavailability, stability and targeted administration of green tea polyphenols²⁰. When combined with chitosan, a natural, biodegradable polymer known for its mucoadhesive and controlled release properties, these iron oxide chitosan nanoparticles (IOCHNP) present an effective delivery platform for oral polyphenol administration²¹. In addition, it has been shown that in both water and GI simulation, the chitosan-coated produced the most delayed total polyphenols release²².

Despite the growing interest in nanoparticle delivery systems, no previous study has comprehensively evaluated the in vitro release characteristics and release kinetics of six major green tea polyphenols (GTPP). Furthermore, the in vivo plasma exposure of gallic acid, catechin, caffeine, epicatechin, EGCG, and theaflavin encapsulated in IOCHNP has not yet been investigated. To our knowledge, this is the first study to assess the feasibility of incorporating these structurally diverse compounds into a single nanoparticle platform and to characterize their release and pharmacokinetic behavior. These specific compounds were selected based on their known bioactivity and poor inherent bioavailability, making them ideal candidates for encapsulation. Therefore, the purposes of this study were, first, to determine the in vitro release characteristic and release kinetic of GTPP (catechin, caffeine, epicatechin, EGCG, gallic acid, and theaflavin) encapsulated in IOCHNP compared with GTPP under simulated gastrointestinal fluid. Secondly, to determine the in vivo plasma exposure of GTPP compound following oral administration of GTPP-IOCHNP and GTPP extracts in plasma samples of Sprague Dawley rats using HPLC.

Materials and methods

Material

Six analytical references standards including: (gallic acid $\geq 98\%$, analytical standard, epicatechin $\geq 98\%$, analytical standard, (-)-epigallocatechin gallate $\geq 98\%$, analytical standard, (+)-catechin $\geq 98\%$, analytical standard, caffeine $\geq 98\%$, analytical standard and theaflavin $\geq 98\%$ (Solarbio Life Sciences, Beijing, China). Acetonitrile, methanol, and water were acquired from (Fisher Scientific in Waltham, Massachusetts, USA), using an HPLC gradient analysis. The simulated intestinal fluid and gastric fluid were purchased from (Solarbio Life Sciences, Beijing, China). The intestinal fluid primarily consists of phosphate buffer and trypsin with a pH of 6.8, whereas the gastric fluid is mainly composed of sodium chloride, dilute hydrochloric acid, and pepsin, with a pH of 3.

Extraction of tea polyphenols (TP) using microwave-assisted extraction

Fresh tea leaves (*Camellia sinensis* L.), the non-clone type, were collected from BOH plantation farms in Cameron Highlands, Pahang, Malaysia. The leaves were then dried for three days at 35 °C in a ventilated drying oven. The dried leaves were powdered using a grinder (Waring, New Hartford, Connecticut). A close microwave assisted extraction system was used to extract the polyphenols from the tea leaves using distilled water (Milestone, Advanced Microwave Labstation, USA) as reported by Serdar, Demir²³. The extraction process was conducted using a regulated 600 W microwave power source at 80 °C for four min of radiation exposure. The extracts were passed through Whatman No. 1 filter paper and stored at -20 °C for later analysis. These filtered samples were designated as GTPP.

Synthesis of iron oxide Chitosan encapsulating green tea polyphenols nanoparticles

Iron oxide nanoparticles were prepared using the co-precipitation method as reported by Barahuie, Dorniani²⁴, with some modifications. Initially, ferrous chloride tetrahydrate ($\text{FeCl}_2 \cdot 4\text{H}_2\text{O}$) and ferric chloride hexahydrate ($\text{FeCl}_3 \cdot 6\text{H}_2\text{O}$) were mixed in a 1:2 molar ratios. A mixture of 0.1 mol FeCl_2 and 0.2 mol FeCl_3 was dissolved using 150 mL of deionized water and stirred at 800 rpm (Heidolph Instruments, model CG-1997, 135 mm, Germany) while heating to 80 °C under a nitrogen gas. Next, 20 mL ammonia was added dropwise, 2 M of sodium hydroxide (NaOH) was added until the solution reached pH 10. After that, 100 mL chitosan solution was added, followed by 100 mL of a solution of tea polyphenols mixture (10 mg/mL in deionized water). Next, 1 mL of a pentasodium tripolyphosphate hexahydrate was added with constant stirring for 1 h. After 1 h, the entire solution was sonicated for 10 min at room temperature and stirred for another 1 h²⁵. The solution was

centrifuged using a Kubota 2810 centrifuge (Japan) for 15 min, 4000 rpm in order to collect the precipitate. Finally, the supernatant obtained from nanoparticle purification process was utilized to assess the encapsulation efficiency and loading capacity of green tea polyphenols. After that, the final precipitate products were oven dried at 70 °C for 18–24 h²⁶. The nanoparticles were quantified based on their mass and were designated as GTPP-IOCHNP.

Analysis of GTPP using HPLC

An Agilent 1100 Series Quaternary LC HPLC with system control and data processing were carried out by a ChemStation 32 Software. A diode-array detector (G1315B) equipped with a 10 mm standard flow cell was employed for detection. A Chromasil C18 analytical column (250 mm × 4.6 mm ID, 5 μm) (Elite, Dalian, China) was utilized to elute the analytes, which were maintained at 30 °C. A mobile phase comprising (A) an aqueous solution of 0.1% formic acid and (B) acetonitrile containing 0.1% formic acid was used to accomplish separation at a flow rate of 1.0 mL/min. For analysis, 20 μL of the sample was injected under a programmed gradient as follows, 10% B (0–5 min), 10–15% B (5–7 min), 15% B (7–10 min), 25% B (10–20 min), 25–40% B (20–25 min), 40% B (25–30 min). A wavelength of 280 nm was used to monitor the effluent. A standard stock solution containing six references standards including, gallic acid, epicatechin, (-)-epigallocatechin gallate, (+)-catechin, caffeine and theaflavin, each at concentration of 1 mg/mL, was prepared using methanol as the solvent. To create the working and spiked standard solution, the stock solution was diluted into 50 μg/mL using the same solvent. A standard calibration curve was constructed by serially diluting the working standard with the same solvent with concentration ranging approximately 1–50 μg/mL²⁷. The resulting solutions were stored at –20 °C until further analysis.

Key validation parameters showed that the developed HPLC method performed satisfactorily. Limits of quantification (LOQ) ranged from 0.964 to 5.663 μg/mL for reference standard solutions and from 1.783 to 9.542 μg/mL for plasma spiked samples. Gallic acid, catechin, caffeine, epicatechin, EGCG, and theaflavin exhibited good linearity ($R^2 \geq 0.95$) across a wide concentration range in reference standard solutions and spiked plasma samples. Recovery percentage was within acceptable limits, ranging from 63.9% to 99.9%²⁸.

Encapsulation efficiency and loading capacity of GTPP

Encapsulation efficiency (EE) and loading capacity (LC) were determined using an indirect quantification method²⁹. The nanoparticle suspension was centrifuged at 4000 rpm for 15 min to separate the nanoparticle precipitate from the unencapsulated (free) drug remaining in the supernatant. The concentration of free drug in the supernatant was then quantified using HPLC analysis. The amount of encapsulated drug was calculated indirectly by subtracting the free drug content from the total drug initially added during formulation. Following the synthesis and purification of GTPP-loaded IOCHNP nanoparticles, the encapsulation efficiency was determined using Eq. (1), while the loading capacity, defined as the amount of drug encapsulated per gram of nanoparticles, was calculated using Eq. (2)³⁰.

$$EE(\%) = (GTPP_{total\ mass} - mass\ of\ free\ GTPP) / GTPP_{total\ mass} \times 100 \quad (1)$$

$$LC(\%) = (GTPP_{total\ mass} - mass\ of\ free\ GTPP) / mass\ of\ recovered\ nanoparticles \times 100 \quad (2)$$

Determination of content of GTPP in GTPP extract and GTPP-IOCHNP

The content of GTPP in the GTPP extract was initially determined by preparing a solution of 100 mg/100 mL, simulating the extract used in the in vitro experiment described in Sect. 2.7. The content of each GTPP was quantified using HPLC analysis. Similarly, the content of GTPP in GTPP-IOCHNP was determined based on the GTPP loading capacity, which determines the amount of GTPP per mg of nanoparticles.

In vitro release of GTPP during simulated Gastrointestinal digestion and extended intestinal incubation

The in vitro digestion procedure was carried out following Minekus, Alminger³¹ with minor modifications. The method consists of two stages, gastric and intestinal stage. In gastric phase, 100 mg samples of GTPP were dispersed in 10 mL of SGF at pH 3. Similarly, 100 mg samples of GTPP-IOCHNP were separately dispersed in 10 mL of SGF at pH 3. After adjusting the pH of the mixtures to 2.5 using 3 M HCl, they were continuously stirred for two h at 37 °C and 300 rpm using a magnetic stirrer. At the end of gastric digestion, 200 μL aliquots were collected, and an equal volume of fresh SGF was added to maintain sink conditions. Samples were centrifuged and subjected to HPLC analysis for GTPP quantification. Prior to initiating the intestinal stage, 1 M NaHCO₃ was added to the gastric digestion solutions to raise the pH level to 7.

In the intestinal digestion stage, SIF was supplemented with ascorbic acid (2 mM) to act as an antioxidant. The addition of ascorbic acid was necessary to protect GTPP from oxidative degradation during the release process, as polyphenolic compounds are highly sensitive to oxidation under physiological conditions³². Following that, the two gastric solutions were mixed with 10 mL of SIF, as previously indicated. The two solutions were continuously stirred at 37 °C. A supernatant aliquot 200 μL were taken after 5, 7, 24, and 27 h. To maintain condition, 200 μL of SIF was retained after every sampling point. The samples centrifuged 3000 × g for 10 min and subjected to HPLC analysis for GTPP released quantification³³. The extended time points (24 and 27 h) were intended to characterize the in vitro release kinetics of GTPP from the nanoparticle formulation under intestinal conditions. Standard kinetic models (zero-order, first-order, Weibull, and Korsmeyer–Peppas) were fitted to the release data using R software. These models follow established mathematical formulations that are widely reported³⁴.

The formula below was utilized to determine the release percentage of GTPP in digestive fluid:

$$\text{Release (\%)} = \text{Cumulative amount of GTPP release in digestive fluid} \div \text{initial total amount of GTPP} \times 100 \quad (3)$$

Cumulative amount of GTPP release denotes the quantity of GTPP (in milligrams) released at time (t), whereas initial total amount of GTPP denotes the total amount of GTPP (in milligrams) inside the nanoparticles.

In vivo analysis

Animals and experimental design

Male Sprague Dawley rats weighing 180–200 g and 6 weeks of age were purchased from A Sapphire Enterprise, Seri Kembangan, Selangor, Malaysia. Rats were acclimated for seven days and fed regular rat chow according to the AIN 76 - A guideline. The rats were sorted into two groups: GTPP group and GTPP-IOCHNP groups. The animals fasted overnight (food but not water) prior to treatment. Using oral gavage, treatment groups were given a single dose of 200 mg/kg BW GTPP and GTPP-IOCHNP, the treatment period was 24 h. The dose used in the current in vivo analysis was selected based on previously published toxicological assessments and safety evaluations. A safe intake limit of 338 mg EGCG/day for adults with normal liver function has been identified for solid formulations, while an Observed Safe Level (OSL) of up to 704 mg/day may be considered for green tea preparations consumed in beverage form^{35,36}. Blood was collected from the retro-orbital plexus, and the plasma was separated and stored in EDTA tubes for in vivo analysis. All experimental procedures were reviewed and approved by the Institutional Animal Care and Use Committee (IACUC) of Universiti Putra Malaysia (AUP No: UPM/IACUC/AUP-R052/2020). All methods were carried out in accordance with the relevant guidelines and regulations for the care and use of laboratory animals and are reported in compliance with the ARRIVE guidelines.

Plasma sample Preparation

An Eppendorf tube with 10 μL of a 20% vitamin C solution was filled with 200 μL of rat plasma that had been thawed at room temperature. The resulting mixture was subjected to two successive extractions using 400 μL of ethyl acetate, involving vortex mixing for 30 s followed by centrifugation at $3000 \times g$ for 10 min at 4 °C. The upper organic phase was transferred to a separate tube and dried by evaporation under gentle stream of nitrogen at 50 °C using water bath. After dissolving the residue in 100 μL of 10% CH_3CN solution, the mixture was centrifuged at $3000 \times g$ for 10 min at 4 °C. An analysis was conducted using an HPLC with a 60 μL sample of the supernatant. According to the method in Sect. 2.4. Plasma concentrations were calculated from spiked standard calibration curve and relative plasma concentration percentage was calculated based on Eq. 4.

$$\text{Relative plasma concentration (\%)} = \text{GTPP plasma Conc.} (\mu\text{L/mL}) \div \text{initial Conc. of GTPP} (\mu\text{L/mL}) \times 100 \quad (4)$$

Statistical analysis

The SPSS 28.0 version was used to analyse the data using the student's t-test. The results were expressed as mean \pm standard deviation. When *p* value was less than 0.05, statistical significance was considered. R software version 4.4.1 was employed for the analysis of in vitro release kinetics modeling. The software was used to compute the correlation coefficients (R^2) for various kinetic models, including zero order, first order, Weibull models and Korsmeyer Peppas, as well as to generate corresponding visualizations of the release profiles.

Results and discussion

Encapsulation efficiency and loading capacity

The GTPP-IOCHNP nanoparticles were initially characterized and confirmed to possess a crystalline structure, with X-ray diffraction (XRD) analysis showing successful coating of the iron oxide–chitosan surface with GTPP at 2θ angles ranging from 20° to 80° and a mean crystallite size of 6.78 ± 1.03 nm. Fourier-transform infrared spectroscopy (FTIR) and transmission electron microscopy (TEM) further confirmed the presence of GTPP and revealed a mean particle size of 8.82 ± 1.79 nm, respectively.

Metal oxide and magnetic nanoparticles possess unique characteristics, such as the ease modification of their surface (compatibility, selectivity and effective regulation of drug release mechanisms)³⁷. The surface positive charge properties of IONP play a significant role in the physical stability and effects the interaction of IONP with the biological system and their safety³⁸. Variety of synthesis techniques such as physically, chemically and biosynthesis technique, resulting in IONP with sizes ranging from 1 to 120 nm³⁹. Nanoparticles with sizes 15–100 nm are optimal due to their long bloodstream circulation times, enabling them to reach various organs and targets. The surface of IONP can be coated with various organic compounds such as chitosan more biocompatible and prevents their aggregation and oxidation⁴⁰.

Additionally, encapsulation efficiency (EE) describes the amount of active ingredients encapsulated within the particles. This parameter is influenced by the encapsulation method, the initial concentration of active compounds, and various experimental conditions, such as pH, ionic strength, and the molecular characteristics of the encapsulated substances. Loading capacity (LC) denotes the particles' total ability to encapsulate the active principle. This capacity is influenced by the structural characteristics and the physical and chemical properties of the material as well as by variables inherent to the manufacturing process³⁰.

Table 1 shows the LC and EE values for green tea polyphenols encapsulated in IOCHNP, determined using Eqs. 1 and 2. The nanoparticles exhibited favorable EE values, notably 80%, 90%, and 83% for gallic acid, catechin, and theaflavin, respectively. Conversely, caffeine, epicatechin, and EGCG displayed lower EE values at 46%, 50%, and 53%, respectively.

The high encapsulation efficiency (EE) observed for GTPP-IOCHNP in this study underscores the potential advantages of chitosan coated iron oxide nanoparticles (IONP) over other coating materials commonly employed for polyphenol delivery. When compared to previously reported systems, the GTPP-IOCHNP formulation

GTPP	Encapsulation efficiency (% ± SD)	Loading capacity (mg/100 g ± SD)
Gallic Acid	80.80 ± 0.075	127.00 ± 0.004
Catechin	90.94 ± 0.764	270.00 ± 0.009
Caffeine	46.34 ± 0.885	72.00 ± 0.002
Epicatechin	50.07 ± 2.143	100.00 ± 0.002
EGCG	53.78 ± 1.705	60.00 ± 0.001
Theaflavin	83.26 ± 13.333	136.00 ± 0.023

Table 1. Encapsulation efficiency and loading capacity of green tea polyphenols iron oxide Chitosan nanoparticles (GTPP-IOCHNP). EGCG: Epigallocatechin Gallate. GTPP: Green Tea Polyphenols. SD: Standard Deviation.

demonstrated superior encapsulation performance. For instance, catechin loaded nanoparticles coated with hydroxyapatite and sodium alginate achieved an EE of 81.25%, as reported by Nobahari, Shahanipour⁴¹, while polyethylene glycol (PEG) coated nanoparticles encapsulating gallic acid exhibited a markedly lower EE of 35% Rosman, Saifullah⁴². The enhanced encapsulation efficiency can be ascribed to multiple factors: (i) the tri-hydroxyl groups on the benzene ring have high reducing potential and low O-H bond dissociation enthalpy, (ii) the bulky group the benzene ring in gallic acid potentially obstructing chitosan's intra- and intermolecular hydrogen bonding networks; (iii) the hydroxyl and carboxyl groups multifunctional hydrophilicity; and (iv) the presence of a carboxylic acid group that facilitates conjugation with chitosan⁴³. Furthermore, the primary mechanisms of the chemical interactions between polyphenols and iron oxide that are essential for the effectiveness of encapsulation are redox reactions, in which polyphenols act as reducing agents for iron oxides, and chelation, in which polyphenolic hydroxyl groups coordinate with iron ions. The nature of these interactions is influenced by factors such as iron's oxidation state (Fe^{2+} or Fe^{3+}), the polyphenol's structural characteristics, and the pH of the surrounding environment all affect the nature of these interactions⁴⁴. These processes contribute to the polyphenols form protective shells or stable polyphenol iron oxide complexes, which improves the stability and modifies the release profile of the encapsulated compounds⁴⁵.

Notably, the encapsulation efficiency of theaflavin in the present GTPP-IOCHNP system reached 83.26%, significantly surpassing that of alternative inorganic nanocomplexes such as gold nanoparticles (AuNPs), which have been reported to achieve an EE of only 47%. Maity, Chatterjee⁴⁶, Cai, Liu⁴⁷ attributed the improved EE to the synergistic effect of the chitosan iron oxide composite matrix, which offers enhanced interactions and stabilization of theaflavin molecules during nanoparticle formation. The encapsulation efficiency (EE %) of gallic acid and theaflavin was higher than that of the other GTPP, which may be partly explained by their relatively greater initial amounts present in the GTPP-IOCHNP formulation (Table 3).

Low EE of EGCG, caffeine and epicatechin can be attributed to several factors. For instance, Echeverri-Cuartas, Agudelo³⁰ proposed that during the synthesis of iron oxide chitosan nanoparticles (IOCHNP), epigallocatechin gallate (EGCG) and water molecules are encapsulated within the iron coordination sphere due to the strong coordination interactions between Fe^{3+} ions and chitosan. Furthermore, caffeine's low encapsulation efficiency is due to its water affinity and the pH of the chitosan solution⁴⁸. Additionally, the EE % was greatly decreased when the pH of the chitosan solution was raised because the CS molecules were less likely to protonate at higher pH values. Low EE % is also attributed to the hydrophilic nature and small molecular weight of caffeine, leading to its preferential partitioning into aqueous phase rather than entrapment in chitosan nanoparticle⁴⁸. Moreover, factors such as chitosan concentration play a significant role in the efficiency of caffeine. An increase in chitosan concentration enhances the availability of protonated chitosan ($-NH_3^+$) in the system. These findings are consistent with the results reported by Abosabaa, ElMeshad⁴⁹, which confirmed that a decrease in EE % was associated with the use of lower chitosan concentrations.

The loading capacity results for all GTPP samples in this study were considered low. The reduced LC observed for gallic acid and catechin can be attributed to their molecular characteristics, as both are small and water soluble compounds approximately 11.5 mg/mL for gallic acid and 25.5 mg/mL for catechin^{50,51}. Their encapsulation is limited due to partitioning between the nanoparticle matrix and the surrounding aqueous environment⁵². Several studies have demonstrated that polyphenolic compounds can interact with the chitosan matrix. Specifically, the amide groups in chitosan and the hydroxyl groups in catechin exhibit notable intermolecular interactions. Consequently, the entrapment efficiency of catechin may be reduced as a result of an unfavourable interaction between chitosan matrix and excessive catechin that hinders the formation of chitosan-tripolyphosphate nanoparticles⁵³. Overall, particle size plays a critical role in drug loading capacity. Smaller particles possess a higher total surface area, which facilitates rapid drug release, as a significant proportion of the drug is located on or near the particle surface. Conversely, larger particles, with their greater core volume, are capable of encapsulating higher amounts of drug, leading to more sustained release profile as the drug diffuses gradually from the core⁵⁴.

However, LC results indicated that gallic acid exhibited high percentage, which is consistent with the findings by Iraj et al., 2018⁵⁵. According to the study, the primary mechanism causing the encapsulation of gallic acid is the creation of hydrogen bonds between the iron oxide chitosan nanoparticles and the carboxyl group of gallic acid. Additionally, the strong electrostatic interaction between negatively charged gallic acid and positively charged iron oxide chitosan surfaces plays a crucial role. This pronounced electrostatic attraction enhances drug absorption, thus increasing the gallic acid loading capacity.

In vitro release of GTPP from IOCHNP under simulated Gastrointestinal digestion*In vitro release profile*

In vitro release profile showed that only four polyphenols (gallic acid, catechin, caffeine, and epicatechin) were detectable in SGF and SIF (Fig. 1).

EGCG and theaflavin were not detected, neither in SGF nor in SIF. The low encapsulation efficiency of EGCG likely contributes to its low concentration in the release medium. Limitations in the sampling procedure may have further affected detectability. A more structured sampling strategy followed by collection at consistent time intervals would improve the ability to monitor and detect both theaflavin and EGCG throughout the release process.

Additionally, theaflavin are highly susceptible to degradation, forming naphthoquinone in alkaline solutions, which contributes to their instability. At pH 7.4, approximately 34.8% of theaflavin degraded after 8 h of incubation. When the pH was elevated to 8.5 the degradation rate increased with 78.4% of theaflavin degraded within just 2 h of incubation⁵⁶. These findings underscore the need for further research into stabilization strategies, such as the co loading of antioxidants, to enhance the applicability of theaflavins in drug delivery systems. Moreover, the incorporation of antioxidants or stabilizing agents into simulated intestinal fluid may offer additional protection, effectively minimizing oxidative degradation following the release of theaflavins.

The cumulative release of gallic acid, catechin, caffeine, and epicatechin in SGF was lower in GTPP-IOCHNP compared to GTPP, suggests that gallic acid, catechin, caffeine and epicatechin encapsulated by IOCHNP can be well protected in gastric fluid⁵⁷. While it released in a higher quantity in SIF imply pH-controlled release of these polyphenols. The maximum GTPP release rate following gastric fluid digestion was less than 8%, indicating that GTPP-IOCHNP could efficiently postpone the release of GTPP in the stomach and move more GTPP into the

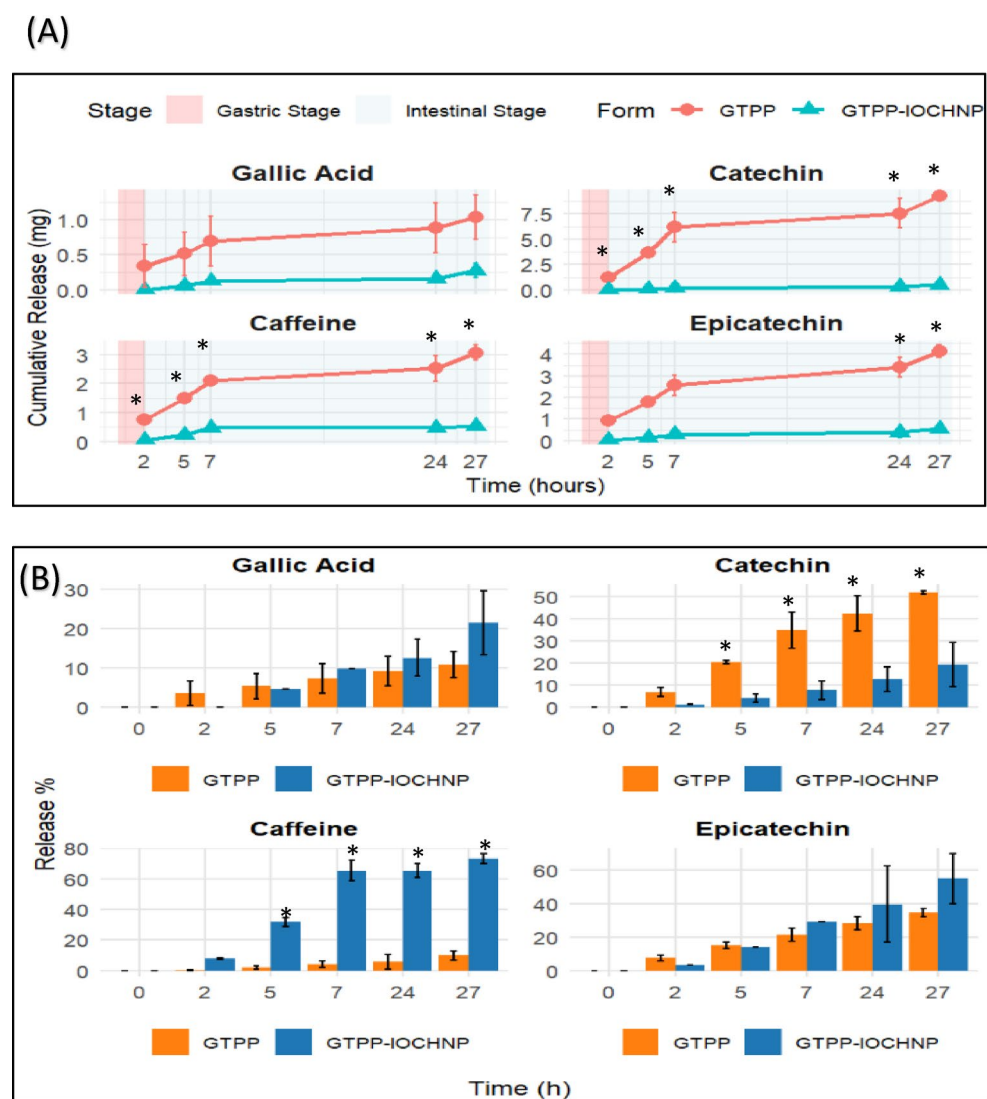


Fig. 1. Cumulative release profiles of Gallic acid, Catechin, Caffeine and Epicatechin in GTPP and GTPP-IOCHNP (A), Release percentage (%) of GTPP and GTPP-IOCHNP (B) in simulated gastric and intestinal fluids at 37 °C for 2, 5, 7, 24 and 27 h. Data are mean \pm SD, * $p < 0.05$ by comparing GTPP with GTPP-IOCHNP.

small intestine⁵⁸. Moreover, Hu, Wang⁵⁹ explained that the release of GTPP from the nano carrier are dependent upon pH levels. The controlled release profile of GTPP from nanoparticles can be effectively modulated by adjusting the GTPP grafting ratios within the IOCHNP. This adjustment reduces the strong repulsive forces among the highly protonated amino groups in chitosan under strongly acidic conditions, thereby decreasing nanoparticle swelling and subsequently slowing the release of the encapsulated payload. Conversely, the release profile of the payloads from the GTPP-IOCHNP could be modified through changing the GTPP grafting ratio, which would favor the controlled release of the contents at alkaline media where chitosan exhibits reduced protonation.

In SIF, the duration of the intestinal digestion in this study does not fully correspond to physiological small intestinal transit, which typically occurs within 2–6 h³¹. In this study, the extended incubation periods (7–27 h) used to assess the sustained release and stability of GTPP from the nanoparticle formulation under intestinal conditions. Therefore, the cumulative release of catechin, caffeine, and epicatechin from GTPP-IOCHNP was consistently and significantly lower than from GTPP throughout the entire SIF period (Fig. 1A). In contrast, gallic acid release from GTPP-IOCHNP was slightly lower but not significantly different from GTPP (Fig. 1A). During the first 2 h, which corresponds to physiologically relevant small intestinal transit, the GTPP-IOCHNP cumulative release of epicatechin, gallic acid, catechin, and caffeine increased sharply, followed by a reduction in release rate and delay at 7 h. Beyond the 5 h intestinal digestion window, extended incubation in SIF (7–27 h) was performed to evaluate long term release and nanoparticle stability. Under these conditions, the cumulative release increased again after 24 h, continuing up to 27 h indicating the sustain released of polyphenols from GTPP-IOCHNP. In comparison to GTPP, the cumulative release followed a consistent rate throughout the entire SIF period (Fig. 1A). The observed biphasic release behavior of GTPP-IOCHNP may be attributed to the adsorption of polyphenols onto the nanoparticle shell, which contributes to the initial burst release. Additionally, the hydrophobic chitosan layer coating the iron oxide nanoparticles may restrict drug diffusion from the core, thereby accounting for the delayed and sustained release phase⁶⁰.

Compared to GTPP, the GTPP-IOCHNP formulation exhibited a reduced release percentage of gallic acid, catechin, caffeine, and epicatechin in SGF (Fig. 1B). In SIF, the cumulative release of gallic acid and epicatechin after 27 h was slightly higher for GTPP-IOCHNP than for GTPP, though the difference was not statistically significant ($P > 0.05$). In contrast, significant increase in caffeine release ($p < 0.05$) was observed in GTPP-IOCHNP group. However, catechin showed a significantly lower release from the nanoparticle formulation.

Among all compounds, caffeine exhibited the highest release percentage, followed by epicatechin, with release values of approximately 73% and 55%, respectively (Fig. 1B). The observed sustained release may be attributed to the presence of hydroxyl and amino groups on the chitosan surface. These groups primarily attach to the surface of nanoparticles, reducing surface voids and pore blockage, lowering penetration and slowing down the rate at which caffeine is released. On the other hand, IONP play a role in magnetic orientation, magnetic nanocaffeine carriers can carry caffeine for long distances by using an external magnetic field. These outcomes made it abundantly evident that the iron oxide containing chitosan produced a barrier system that allowed for the continuous release of caffeine⁶¹. According to Hassan et al., 2018⁶² self-assembled chitosan nanoparticles loaded with caffeine showed a relatively limited release profile, with a cumulative release of only 50–60% over 72 h. In contrast, GTPP-IOCHNP system achieved encapsulation efficiency (EE %) of 46% and a cumulative release of 72.3% over 72 h, indicating a more efficient and sustained release. Overall, the release of gallic acid, caffeine, and epicatechin from GTPP-IOCHNP in simulated gastrointestinal fluid was increased by approximately 1.97-fold, 2.21-fold, and 1.59-fold, respectively, compared to GTPP.

In vitro GTPP release kinetics from GTPP-IOCHNP

The *in vitro* cumulative release of GTPP from the iron oxide chitosan nanoparticles was analyzed using five kinetic models (zero-order, first-order, Higuchi, Korsmeyer–Peppas, and Weibull) to provide an exploratory assessment of release behavior⁶³. Table 2 shows the correlation coefficients (R^2) obtained from different kinetic models used as the main factors in choosing the best fit model. However, given the limited number of sampling points, particularly between 7 h and 24 h, these results were interpreted with caution. The modeling analysis is therefore intended to offer preliminary, descriptive insights into possible release mechanisms rather than definitive mechanistic characterization. Future studies with denser sampling schedules are required to confirm these observations. As demonstrated by the results, the Higuchi model exhibited the highest coefficient of determination (R^2) for both gallic acid and epicatechin, surpassing that of the other assessed kinetic models. This suggests that diffusion may contribute to the release of these polyphenols from the nanoparticles, consistent with Fickian-type transport (Fig. 2a). Furthermore, the lower Higuchi release rate constant (k) observed for gallic acid, relative to epicatechin, indicates a slower apparent diffusion rate and a more sustained release profile. This trend may partly explain the lower cumulative release percentage of gallic acid, which reached approximately

Polyphenols	Zero	First	Higuchi	Korsmeyer-Peppas	Weibull
Gallic acid	0.928	0.936	0.956	0.901	0.945
Catechin	0.945	0.938	0.949	0.969	0.902
Caffeine	0.730	0.786	0.816	0.799	0.935
Epicatechin	0.972	0.741	0.990	0.940	0.980

Table 2. Statistical R^2 parameters of (gallic acid, catechin, caffeine and epicatechin) from GTPP-IOCHNP in simulated gastric and intestinal fluids.

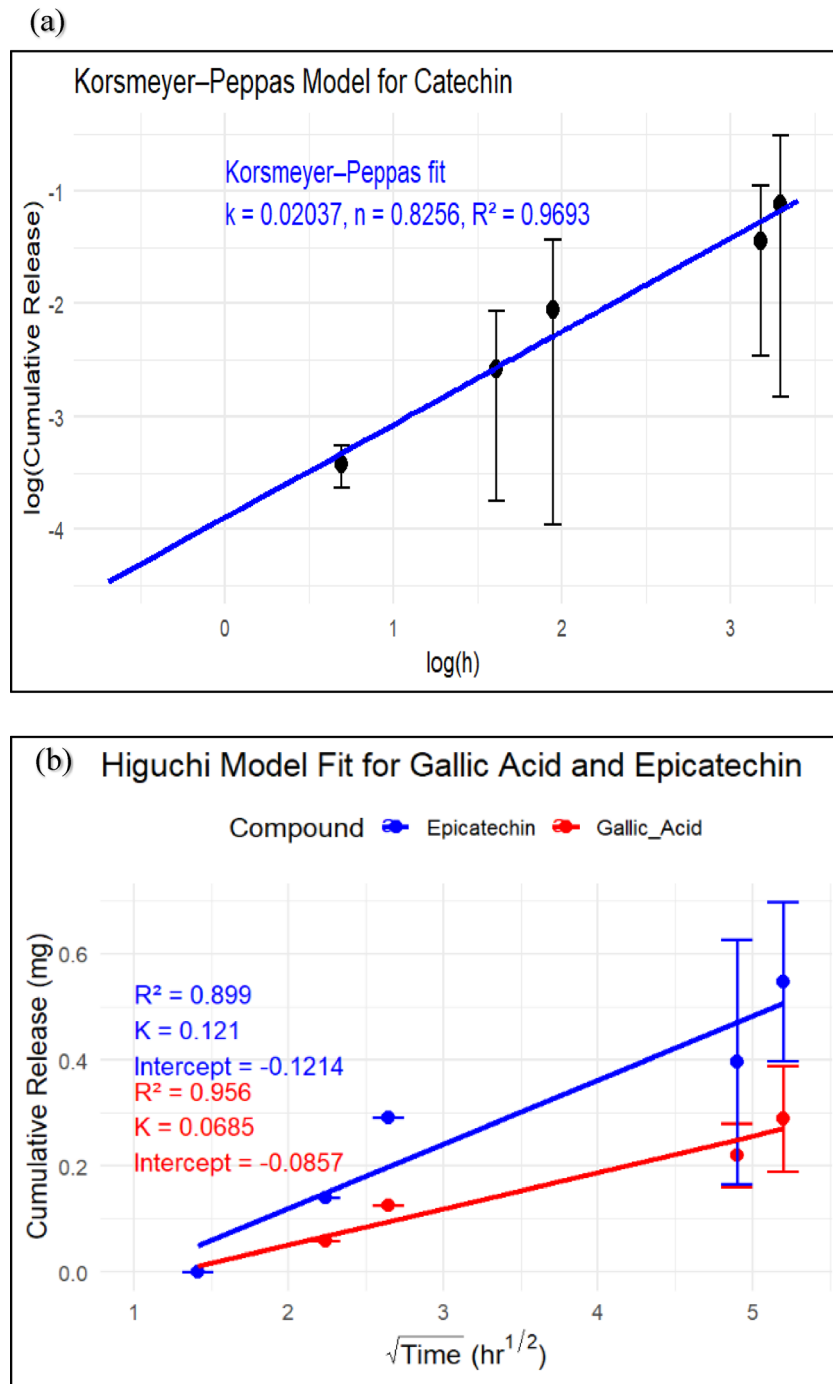


Fig. 2. Release kinetics of gallic acid, epicatechin, caffeine and catechin by Higuchi (a), Korsmeyer–Peppas (b) and Weibull model(c) in simulated gastrointestinal fluid.

22% after 27 h. Additionally, the incomplete release of gallic acid from GTPP-IOCHNP can be tentatively attributed to the basic characteristics of the ion exchange reaction mechanism. Specifically, the loaded anions are not entirely exchangeable due to the equilibrium limitations of the system. However, the gradual removal of the chitosan based organic layer contributed to a sustained release of the encapsulated compound as chitosan layer erodes slowly at higher pH. These findings suggest that GTPP-IOCHNP exhibits promising potential as a drug delivery system, offering controlled and sustained release properties for gallic acid⁶⁴.

The release kinetics of catechin from GTPP-IOCHNP nanoparticles exhibited strong correlation with the Korsmeyer Peppas model, as evidenced by a high coefficient of determination ($R^2 = 0.97$). Analysis of the release exponent (n) revealed values between 0.43 and 0.85, indicating an anomalous (non-Fickian) diffusion mechanism (Fig. 2b). This intermediate release behavior indicates a complex mechanism involving both diffusion-controlled drug release and polymer relaxation or swelling phenomena. Such a combination of

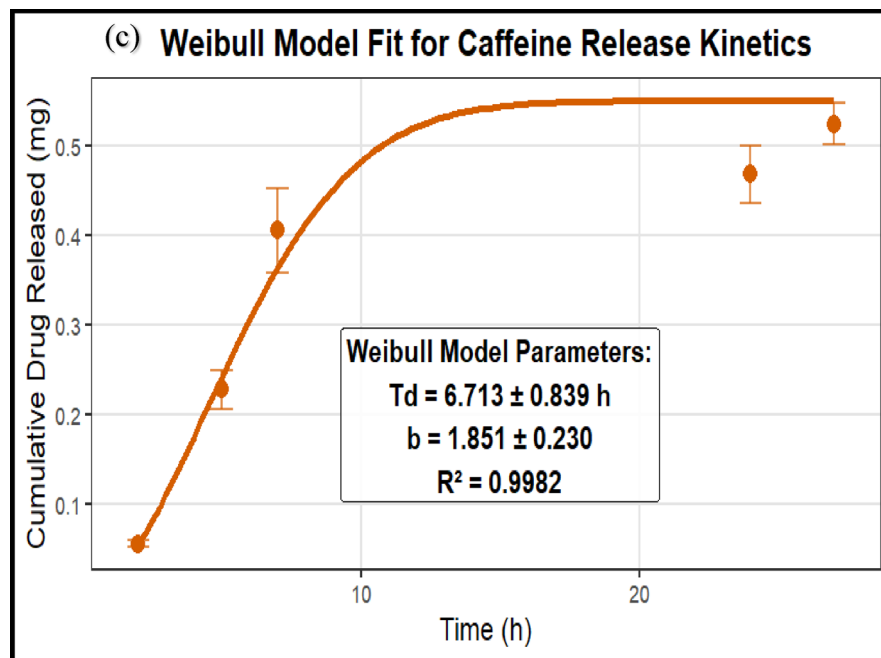


Fig. 2. (continued)

processes may account for the relatively low cumulative release of catechin, which was approximately 20%. The high encapsulation efficiency of catechin (90%) along with their observed release characteristics, are hallmarks of optimized hydrophilic polymer matrices. Drug release is subject to simultaneous physical and chemical processes, including polymer hydration, solvent penetration, drug dissolution, and gradual matrix degradation. The n values confirm a deviation from classical Fickian diffusion, reflecting the characteristic behavior of swell able polymeric nanocarriers with high drug loading capacity⁶⁵. Compared to the findings of Singh et al., 2017⁶⁶ where catechin loaded PLA-PEG nanoparticles followed the Hixson Crowell model and exhibited a Fickian release profile, the iron oxide chitosan nanoparticles developed in the present study demonstrate a distinct and novel release mechanism. Specifically, the release behavior observed suggests that both diffusion and polymer matrix dynamics, such as swelling and erosion, contribute to catechin release, thereby offering greater tunability and control. This contrasts with PLA based systems, which primarily rely on hydrolytic degradation for drug release.

The release profile of caffeine from iron oxide chitosan nanoparticles GTPP-IOCHNP was best described by the Weibull model, as evidenced by the coefficient of determination (R^2) values approaching unity (Fig. 2c). This observation suggests that the release behavior is significantly influenced by the physicochemical interactions between caffeine and the nanoparticle matrix, particularly the iron oxide core. The pronounced electrostatic interactions between caffeine and the iron oxide component of the nanoparticles may have further contributed to this release pattern⁶⁷. Moreover, the Weibull shape parameter (b) was greater than 1, indicating a complex release mechanism involving multiple contributing factors such as diffusion, matrix erosion, and polymer swelling⁶⁸. A study by Hodali et al., 2016⁶⁹ investigated caffeine loading into micro and nanoparticles of mesoporous silicate materials and reported that caffeine release from nanoparticles was faster than from microparticles, with diffusion identified as the predominant release mechanism across all systems. In contrast, the GTPP-IOCHNP formulation developed in the present study exhibited a more sustained release profile of caffeine. Notably, the release kinetics were best described by the Weibull model, suggesting a more complex and flexible release behavior governed by a combination of diffusion and polymer matrix relaxation or erosion rather than being limited to simple Fickian diffusion. This feature underlines the novelty and multifunctionality of GTPP-IOCHNP. It not only enhances release characteristics but also opens up new possibilities for targeted and controlled caffeine delivery in therapeutic applications. Nonetheless, these mechanistic interpretations should be regarded as preliminary, given the limited sampling density, and require confirmation in future studies with more detailed release profiles.

Relative plasma exposure of GTPP after oral administration in rat plasma samples

The initial concentration of the gavage solutions was analyzed prior to the oral administration of GTPP extract and GTPP-IOCHNP formulations. Subsequently, the plasma concentrations (Table 3) and relative plasma conc. (%) (Fig. 3) of catechin, caffeine, gallic acid, epicatechin, EGCG, and theaflavin were measured in rat plasma following administration. These evaluations were conducted to assess the in vivo plasma exposure of GTPP in both free and nanoparticle encapsulated forms.

The plasma concentrations of polyphenols observed after administering GTPP differed significantly from those following administration of GTPP-IOCHNP ($p < 0.05$). Notably, for most compounds, the relative plasma

	GTPP	GTPP-IOCHNP
Polyphenols	Concentration ($\mu\text{g/mL}$)	Concentration ($\mu\text{g/mL}$)
Gallic Acid	7.03 ± 1.748^a	5.71 ± 1.284^b
Catechin	3.48 ± 0.189^a	3.08 ± 0.110^b
Caffeine	3.72 ± 2.585^a	2.22 ± 0.259^a
Epicatechin	10.69 ± 0.896^a	6.92 ± 0.779^b
EGCG	3.98 ± 0.582^a	3.66 ± 0.163^a
Theaflavin	15.60 ± 2.983^a	9.06 ± 2.095^b

Table 3. Plasma concentration of polyphenols in rats supplemented with GTPP and GTPP-IOCHNP. Data presented as Mean \pm SD. Significant at $p < 0.05$ is indicated by different letters (a, b) in the same row. GTPP: Green Tea Polyphenols. GTPP-IOCHNP: Green Tea Polyphenols-Iron Oxide Chitosan Nanoparticles. EGCG: Epigallocatechin Gallate.

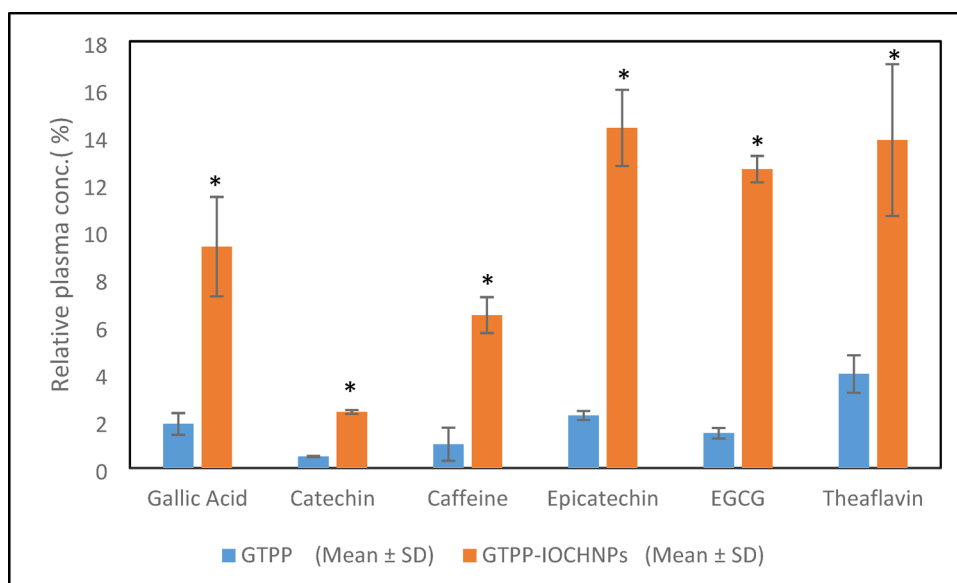


Fig. 3. Relative plasma concentration percentage of polyphenols in rat supplemented with GTPP and GTPP-IOCHNP. Data is displayed as Mean \pm SD, $n = 3$, * indicates significant at $p < 0.05$ between GTPP and GTPP-IOCHNP.

levels were higher in the GTPP-IOCHNP group, indicating that the iron oxide chitosan nanoparticle formulation improved systemic exposure to gallic acid, catechin, caffeine, epicatechin, EGCG, and theaflavin.

Findings showed that theaflavin, epicatechin, gallic acid and EGCG encapsulated in GTPP-IOCHNP exhibited the highest plasma concentrations compared with caffeine and catechin. Analysis of matrix effect, recovery percentages, and encapsulation efficiencies found compatibility in these compounds due to their high encapsulation efficiencies. In contrast, the lowest plasma concentration was found for caffeine and catechin in GTPP-IOCHNP as shown in Table 3. Analysis of low encapsulation efficiency for caffeine provides an explanation for the decreased plasma concentrations of these substances.

In the case of catechin, a study conducted by Kim, Lee⁷⁰ reported low plasma concentrations, which were accompanied by a temporal increase in epigallocatechin and epicatechin levels. Peak plasma concentrations of these metabolites were observed approximately one day after administration, showing a threefold increase. The researcher explains that the reason for the decrease in catechins in plasma may be due to the conversion of catechins found in tea into unspecified metabolites. Furthermore, the encapsulation efficiency results revealed that catechin exhibited the highest encapsulation efficiency among the compounds tested within the GTPP-IOCHNP formulation. Interestingly, in rat plasma, catechin had the lowest concentration despite this effective encapsulation. This findings are in line with those of Kim, Lee⁷⁰ and Baba, Osakabe⁷¹, showing that encapsulation of catechin in IOCHNP increases the conversion of catechin to metabolites such as epicatechin and EGCG, which in turn causes a slight decrease in catechin levels in rat plasma.

One important finding in our investigation was that EGCG's plasma concentration percentage was significantly less than epicatechin's. According to Lubet, Yang⁷², EGCG's bioavailability in rats, mice, and humans is significantly lower than epicatechin's due to its complex chemical structure, consists of eight phenolic groups and a molecular weight of nearly 450. Epicatechin and EGCG plasma exposure percentage was significantly

higher in the GTPP-IOCHNP group, by approximately 6.5- and 8.5- fold, respectively, compared with GTPP. This enhancement may be attributed to the incorporation of chitosan during the iron oxide nanoparticle formulation process. For example, previous studies have shown that chitosan nanoparticles loaded with EGCG improve intestinal permeability across Caco-2 cells, leading to greater absorption of EGCG. The increased exposure of EGCG to the jejunum has been associated with the stabilizing effect of chitosan nanoparticles, which protect polyphenols from degradation and facilitate their transport⁷³.

The results showed that encapsulating EGCG, epicatechin, and catechin within iron oxide chitosan-based nanoparticles led to an increase in plasma levels percentage for all three compounds. The magnitude of enhancement followed the order EGCG > epicatechin > catechin, corresponding to 8.5-fold, 6.5-fold, and 4.8-fold increases, respectively. This indicates that EGCG exhibited greater stability when encapsulated within iron oxide-chitosan nanoparticles compared to epicatechin and catechin. This finding is consistent with a study conducted by Chanphai and Tajmir-Riahi⁷⁴, which showed that a number of factors affect the tea catechins' ability to bind with chitosan nanoparticles. Hydrophilic, hydrophobic and hydrogen bonding interactions lead to polyphenol polymer conjugation; the order of stability is EGCG > epicatechin > catechin.

Regarding gallic acid, the analysis conducted in this study revealed that administration of gallic acid-IOCHNP resulted in a nearly 5-fold increase in plasma gallic acid levels compared to the free form (Fig. 3). The enhancement may be attributed to the high encapsulation efficiency of gallic acid within the IOCHNP system. These results highlight that gallic acid-IOCHNP potential as efficient gallic acid carriers, which has implications for several therapeutic uses. Saleh, Ragab⁷⁵ demonstrated that iron oxide carboxymethyl chitosan gallic acid nanoparticle formulations selectively induce apoptosis in cancer cells, while exhibiting minimal effects on normal cells. This selective targeting of cancer cells holds significant promise for minimizing damage to healthy cells, which indicates that using iron oxide nanoparticle improves the effectiveness and the safety profile of cancer treatment modalities.

Encapsulation of theaflavin within IOCHNP markedly enhanced its stability and plasma concentration. The findings demonstrated that the plasma level percentage of theaflavin increased by 3.5-fold when delivered via IOCHNP compared with the free form. This improvement can be attributed to the high encapsulation efficiency of theaflavin, as well as the chitosan-based delivery system, which is expected to enhance the intestinal permeability of theaflavins⁷⁶.

A comparison of the in vivo and in vitro study outcomes revealed difference in epicatechin (EC) plasma level. The in vivo study demonstrated a 6.5-fold increase in EC plasma level, whereas the in vitro assay showed only a 2-fold increase. The in vivo investigation revealed a greater degree of absorption. In vitro assays may produce results that do not fully align with in vivo outcomes, owing to inherent methodological limitations and the simplified nature of the experimental conditions. One major factor is the auto oxidation of epicatechins during in vitro digestion, particularly under simulated small intestinal conditions. Additionally, the alkaline solution used to adjust pH during digestion can further degrade EC, reducing its apparent plasma level. The in vitro simulated digestion assay may not be a reliable indicator of the in vivo oral administration of tea catechins for these reasons⁷⁷.

Conclusion

The encapsulation of GTPP within iron oxide chitosan nanoparticles (IOCHNP) resulted in effective encapsulation efficiencies, with EE % values of 80% for gallic acid, 90% for catechin, and 83% for theaflavin. IOCHNP successfully protected the GTPP from early degradation in gastric fluid and facilitated their release in intestinal fluid. less than 8% of GTPP is released in simulated gastric fluid (SGF), while release was enhanced in simulated intestinal fluid (SIF), reaching up to 70% for caffeine within the physiologically relevant 5 h intestinal digestion. extended incubation in SIF (5–27 h) demonstrated the sustained release capacity of the nanoparticle system. Release kinetics revealed that gallic acid and epicatechin followed the Higuchi model, indicating Fickian diffusion, while catechin exhibited non Fickian release behavior via the Korsmeyer Peppas model. Caffeine followed the Weibull model, suggesting a more complex release mechanism. Notably, the relative plasma concentrations of EGCG, epicatechin, and catechin increased significantly by 8.5-, 6.5-, and 4.8-fold, respectively, indicating that encapsulation markedly enhanced their systemic exposure in vivo.

The well-dispersed, smaller nanoparticles are advantageous for biomedical applications, particularly in drug delivery, where smaller particles offer enhanced bioavailability, might demonstrate better penetration through biological barriers, and improved interaction with target cells or tissues. These results support the potential of IOCHNP as a promising nanocarrier system for the oral delivery of polyphenolic compounds.

Data availability

The data that support the findings of this study are available from the corresponding author upon reasonable request.

Received: 19 May 2025; Accepted: 31 December 2025

Published online: 20 January 2026

References

1. Radeva-Ilieva, M., Stoeva, S. & Hvarhanchanova, N. & K.D. Georgiev. Green Tea: Current Knowledge and Issues. *Foods*. **14**, (2025).
2. Zhang, Q. et al. Antimicrobial effect of tea polyphenols against foodborne pathogens: A review. *J. Food. Prot.* **84**, 1801–1808 (2021).
3. Saric, S., Notay, M. & Sivamani, R. K. Green tea and other tea polyphenols: effects on Sebum production and acne vulgaris. *Antioxidants* **6**, 2 (2017).
4. Karas, D. & Ulrichová, J. & K. Valentová. Galloylation of polyphenols alters their biological activity. *Food Chem. Toxicol.* **105**, 223–240 (2017).

5. Yin, Z. et al. Improving the stability and bioavailability of tea polyphenols by encapsulations: a review. *Food Sci. Hum. Wellness*. **11**, 537–556 (2022).
6. Lippolis, T., Cofano, M., Caponio, G. R. & De Nunzio, V. & M. Notarnicola. Bioaccessibility and bioavailability of diet polyphenols and their modulation of gut microbiota. *Int. J. Mol. Sci.* **24**, 3813 (2023).
7. Krupkova, O. & Ferguson, S. J. Wuerztz-Kozak. Stability of (-)-epigallocatechin gallate and its activity in liquid formulations and delivery systems. *J. Nutr. Biochem.* **37**, 1–12 (2016).
8. Cai, Z. Y. et al. Bioavailability of Tea Catechins and Its Improvement. *Molecules*. **23**, 2346 (2018).
9. Liu, B. & Kang, Z. & W. Yan. Synthesis, Stability, and Antidiabetic Activity Evaluation of (-)-Epigallocatechin Gallate (EGCG) Palmitate Derived from Natural Tea Polyphenols. *Molecules*. **26**, 393 (2021).
10. Konishi, Y., Kobayashi, S. & Shimizu, M. Transepithelial transport of p-coumaric acid and Gallic acid in Caco-2 cell monolayers. *Biosci. Biotechnol. Biochem.* **67**, 2317–2324 (2003).
11. Fujiki, H., Sueoka, E. & Watanabe, T. & M. Suganuma. Synergistic enhancement of anticancer effects on numerous human cancer cell lines treated with the combination of EGCG, other green tea catechins, and anticancer compounds. *J. Cancer Res. Clin. Oncol.* **141**, 1511–1522 (2015).
12. Qi, C. et al. A comprehensive review of nano-delivery system for tea polyphenols: Construction, applications, and challenges. *Food Chemistry: X*. **17**, 100571 (2023).
13. Kulandaivelu, K. & Mandal, A. K. A. Improved bioavailability and pharmacokinetics of tea polyphenols by encapsulation into gelatin nanoparticles. *IET Nanobiotechnol.* **11**, 469–476 (2017).
14. Li, H. et al. Encapsulation of polyphenols in pH-responsive micelles self-assembled from octenyl-succinylated curdlan oligosaccharide and its effect on the gut microbiota. *Colloids Surf., B*. **219**, 112857 (2022).
15. Istenič, K. & Cerc, R. Korošec, & N. Poklar Ulrih. Encapsulation of (-)-epigallocatechin gallate into liposomes and into alginate or Chitosan microparticles reinforced with liposomes. *J. Sci. Food. Agric.* **96**, 4623–4632 (2016).
16. An, J., Liu, M., Din, Z. & Xie, F. Cai. Toward function starch nanogels by self-assembly of polysaccharide and protein: from synthesis to potential for polyphenol delivery. *Int. J. Biol. Macromol.* **247**, 125697 (2023).
17. Grodzicka, M. et al. Heterofunctionalized polyphenolic dendrimers decorated with caffeic acid: Synthesis, characterization and antioxidant activity. *Sustainable Mater. Technol.* **33**, e00497 (2022).
18. Wang, X. et al. ROS-responsive capsules engineered from green tea polyphenol–metal networks for anticancer drug delivery. *J. Mater. Chem. B*. **6**, 1000–1010 (2018).
19. Tran, H. V. et al. Multifunctional iron oxide magnetic nanoparticles for biomedical applications: A review. *Materials (Basel)*. **15**, 503 (2022).
20. Zhang, J. & Zhang, T. & J. Gao. Biocompatible iron oxide nanoparticles for targeted cancer gene therapy: A review. *Nanomaterials (Basel)*. **12**, 3323 (2022).
21. Di Santo, M. C., D' Antoni, C. L., Domínguez Rubio, A. P., Alaimo, A. & Pérez, O. E. Chitosan-tripolyphosphate nanoparticles designed to encapsulate polyphenolic compounds for biomedical and pharmaceutical applications—A review. *Biomed. Pharmacother.* **142**, 111970 (2021).
22. Li, Q. et al. Fabrication and characterization of Ca(II)-alginate-based beads combined with different polysaccharides as vehicles for delivery, release and storage of tea polyphenols. *Food Hydrocoll.* **112**, 106274 (2021).
23. Serdar, G., Demir, E., Bayrak, S. & M. Sökmen. New approaches for effective microwave assisted extraction of caffeine and catechins from green tea. *Int. J. Secondary Metabolite*. **3**, 3–13 (2016).
24. Barahuie, F. et al. Sustained release of anticancer agent phytic acid from its chitosan-coated magnetic nanoparticles for drug-delivery system. *Int. J. Nanomed.* **12**, 2361–2372 (2017).
25. Khan, M. et al. Pulicaria glutinosa plant extract: a green and eco-friendly reducing agent for the Preparation of highly reduced graphene oxide. *RSC Adv.* **4**, 24119–24125 (2014).
26. Asey, M. N. & Mohd Esa, N. & C.A. Che Abdullah. Synthesis and characterization of magnetic nanoparticles (MNP) and MNP-Chitosan composites. *Malaysian J. Sci. Health & Technology* **4**, 39–44 (2019).
27. Marchelak, A. & Olszewska, M. A. & A. Owczarek. Simultaneous quantification of thirty polyphenols in blackthorn flowers and dry extracts prepared thereof: HPLC-PDA method development and validation for quality control. *Journal of Pharmaceutical and Biomedical Analysis*. **184**, 113121 (2020).
28. Al Awawdeh, S. et al. Analytical method development for polyphenol detection in rat plasma using green Tea-Loaded Chitosan-Iron oxide Nanoparticles. *BioNanoScience*. **16**, 69 (2025).
29. Marques, S. S. & M.A. Segundo. Nanometrics goes beyond the size: assessment of nanoparticle concentration and encapsulation efficiency in nanocarriers. *TRAC Trends Anal. Chem.* **174**, 117672 (2024).
30. Echeverri-Cuartas, C. E. & Agudelo, N. A. Gartner. Chitosan-PEG-folate-Fe(III) complexes as nanocarriers of epigallocatechin-3-gallate. *Int. J. Biol. Macromol.* **165**, 2909–2919 (2020).
31. Minekus, M. et al. A standardised static in vitro digestion method suitable for food – an international consensus. *Food Funct.* **5**, 1113–1124 (2014).
32. Dube, A., Ng, K. & Nicolazzo, J. A. & I. Larson. Effective use of reducing agents and nanoparticle encapsulation in stabilizing catechins in alkaline solution. *Food Chem.* **122**, 662–667 (2010).
33. Yan, S. et al. Non-extractable polyphenols of green tea and their antioxidant, anti- α -glucosidase capacity, and release during in vitro digestion. *J. Funct. Foods*. **42**, 129–136 (2018).
34. Pourtalebi Jahromi, L., Ghazali, M. & Ashrafi, H. A. Azadi. A comparison of models for the analysis of the kinetics of drug release from PLGA-based nanoparticles. *Heliyon* **6**, e03451 (2020).
35. Hu, J., Webster, D., Cao, J. & Shao, A. The safety of green tea and green tea extract consumption in adults – Results of a systematic review. *Regul. Toxicol. Pharmacol.* **95**, 412–433 (2018).
36. Dekant, W., Fujii, K., Shibata, E. & Morita, O. & A. Shimotoyodome. Safety assessment of green tea based beverages and dried green tea extracts as nutritional supplements. *Toxicol. Lett.* **277**, 104–108 (2017).
37. Sidhu, A. & Verma, N. & P. Kaushal. Role of biogenic capping agents in the synthesis of metallic nanoparticles and evaluation of their therapeutic potential. *Frontiers Nanotechnology* **3**, 801620 (2022).
38. Wu, W., Wu, Z., Yu, T. & Jiang, C. Kim. Recent progress on magnetic iron oxide nanoparticles: synthesis, surface functional strategies and biomedical applications. *Sci. Technol. Adv. Mater.* **16**, 023501 (2015).
39. Sankaranarayanan, S. A., Thomas, A., Revi, N. & Ramakrishna, B. & A.K. Rengan. Iron oxide nanoparticles for theranostic applications - Recent advances. *J. Drug Deliv. Sci. Technol.* **70**, 103196 (2022).
40. Yetisgin, A. A., Cetinel, S., Zuvin, M. & Kosar, A. & O. Kutlu. Therapeutic nanoparticles and their targeted delivery applications. *Molecules* **25**, 2193 (2020).
41. Nobahari, M., Shahanipour, K. & Fatahian, S. & R. Monajemi. Evaluation of cytotoxic activity of loaded Catechin into iron oxide nanoparticles coated with sodium alginate and hydroxyapatite against human HT-29 colon adenocarcinoma and breast cancer MCF-7 cells. *Russ. J. Bioorg. Chem.* **49**, 1049–1058 (2023).
42. Rosman, R. et al. Improved anticancer effect of magnetite nanocomposite formulation of GALLIC acid (Fe₃O₄-PEG-GA) against Lung, breast and colon cancer cells. *Nanomaterials* **8**, 83 (2018).
43. Queiroz, M. F., Sabry, D. A., Sasaki, G. L. & Rocha, H. A. O. & L.S. Costa. Gallic Acid-Dextran conjugate: green synthesis of a novel antioxidant molecule. *Antioxidants* **8**, 478 (2019).

44. Cai, W. Q. et al. Reactive oxygen Species-Responsive polymer drug delivery system targeted oxidative stressed colon cells to ameliorate colitis. *ACS Nano*. **19**, 17287–17308 (2025).
45. Pan, Y. et al. The interactions of polyphenols with Fe and their application in Fenton/Fenton-like reactions. *Sep. Purif. Technol.* **300**, 121831 (2022).
46. Maity, R. et al. Gold nanoparticle-assisted enhancement in the anti-cancer properties of Theaflavin against human ovarian cancer cells. *Mater. Sci. Engineering: C*. **104**, 109909 (2019).
47. Cai, W. Q. et al. Synergistic effect of lecithin and alginate, CMC, or PVP in stabilizing Curcumin and its potential mechanism. *Food Chem.* **413**, 135634 (2023).
48. Massella, D. et al. Preparation of bio-functional textiles by surface functionalization of cellulose fabrics with caffeine loaded nanoparticles. *IOP Conf. Series: Mater. Sci. Eng.* **460**, 012044 (2018).
49. Abosabaa, S. A., ElMeshad, A. N. & Arafa, M. G. Chitosan nanocarrier entrapping hydrophilic drugs as advanced polymeric system for dual pharmaceutical and cosmeceutical application: A comprehensive analysis using Box-Behnken design. *Polymers (Basel)* **13**, 677 (2021).
50. Ledianasari, S., Warya, Nurjayanti & S. Solubility improvement of Gallic acid in water through cocrystal formation with the solvent-drop grinding method and tartaric acid as co-former. *Pharm. Educ.* **22**, 156–159 (2022).
51. Srinivas, K. & Howard, K. J. W. L. & J. Monrad. Solubility of Gallic acid, Catechin, and Protocatechuic acid in subcritical water from (298.75 to 415.85) K. *J. Chem. Eng. Data*. **55**, 3101–3108 (2010).
52. Dube, A. & Nicolazzo, J. A. & I. Larson. Chitosan nanoparticles enhance the intestinal absorption of the green tea catechins (+)-catechin and (-)-epigallocatechin gallate. *Eur. J. Pharm. Sci.* **41**, 219–225 (2010).
53. Liu, B., Wang, Y., Yu, Q. & Li, D. Li. Synthesis, characterization of catechin-loaded folate-conjugated Chitosan nanoparticles and their anti-proliferative effect. *CyTA - J. Food*. **16**, 868–876 (2018).
54. Javid, A., Ahmadian, S., Saboury, A. A. & Kalantar, S. M. Rezaei-Zarchi. Chitosan-Coated superparamagnetic iron oxide nanoparticles for doxorubicin delivery: synthesis and anticancer effect against human ovarian cancer cells. *Chem. Biol. Drug Des.* **82**, 296–306 (2013).
55. Iraj, S. & Ganji, F. Rashidi. Surface modified mesoporous silica nanoparticles as sustained-release Gallic acid nano-carriers. *J. Drug Deliv. Sci. Technol.* **47**, 468–476 (2018).
56. Shi, M. et al. Beneficial effects of Theaflavins on metabolic syndrome: from molecular evidence to gut Microbiome. *Int. J. Mol. Sci.* **23**, 7595 (2022).
57. Yang, R. et al. Nano-encapsulation of Epigallocatechin gallate in the ferritin-chitosan double shells: simulated digestion and absorption evaluation. *Food Res. Int.* **108**, 1–7 (2018).
58. Li, X., Zhou, P., Luo, Z., Feng, R. & Wang, L. Hohenbuehelia Serotina polysaccharides self-assembled nanoparticles for delivery of Quercetin and their anti-proliferative activities during Gastrointestinal digestion in vitro. *Int. J. Biol. Macromol.* **203**, 244–255 (2022).
59. Hu, B. et al. Polymer nanoparticles composed with Gallic acid grafted Chitosan and bioactive peptides combined antioxidant, anticancer activities and improved delivery property for labile polyphenols. *J. Funct. Foods*. **15**, 593–603 (2015).
60. Li, F. et al. The simultaneous loading of Catechin and Quercetin on chitosan-based nanoparticles as effective antioxidant and antibacterial agent. *Food Res. Int.* **111**, 351–360 (2018).
61. Chen, X. et al. Magnetic and self-healing chitosan-alginate hydrogel encapsulated gelatin microspheres via covalent cross-linking for drug delivery. *Mater. Sci. Engineering: C*. **101**, 619–629 (2019).
62. Hassan, A., Sahudin, S., Hussain, Z. & Hussain, M. Hussain. Self-assembled Chitosan nanoparticles for percutaneous delivery of caffeine: Preparation, characterization and in vitro release studies. *Int. J. App Pharm.* **10**, 172–185 (2018).
63. Manjusha, V., Rajeev, M. R. & Anirudhan, T. S. Magnetic nanoparticle embedded chitosan-based polymeric network for the hydrophobic drug delivery of Paclitaxel. *Int. J. Biol. Macromol.* **235**, 123900 (2023).
64. Dorniani, D. et al. Graphene Oxide-Gallic acid nanodelivery system for cancer therapy. *Nanoscale Res. Lett.* **11**, 491 (2016).
65. Katuwavila, N. P. et al. Alginate nanoparticles protect ferrous from oxidation: potential iron delivery system. *Int. J. Pharm.* **513**, 404–409 (2016).
66. Singh, N. A., Mandal, A. K. A. & Khan, Z. A. Fabrication of PLA-PEG Nanoparticles as Delivery Systems for Improved Stability and Controlled Release of Catechin. *Journal of Nanomaterials*. **2017**, 6907149 (2017).
67. Ahmadi, M., Pourmadadi, M., Ghorbanian, S. A. & Yazdian, F. Rashedi. Ultra pH-sensitive nanocarrier based on Fe₂O₃/chitosan/montmorillonite for Quercetin delivery. *Int. J. Biol. Macromol.* **191**, 738–745 (2021).
68. Lemos, T. S. A., de Souza, J. F. & Fajardo, A. R. Magnetic microspheres based on pectin coated by Chitosan towards smart drug release. *Carbohydr. Polym.* **265**, 118013 (2021).
69. Hodali, H., Rawajfeh, R. & Allababdeh, N. Caffeine loading into Micro- and nanoparticles of mesoporous silicate materials: in vitro release kinetics. *J. Dispers. Sci. Technol.* **38**, 1342–1347 (2017).
70. Kim, S. et al. Plasma and tissue levels of tea catechins in rats and mice during chronic consumption of green tea polyphenols. *Nutr. Cancer*. **37**, 41–48 (2000).
71. Baba, S. et al. In vivo comparison of the bioavailability of (+)-Catechin, (-)-Epicatechin and their mixture in orally administered rats. *J. Nutr.* **131**, 2885–2891 (2001).
72. Lubet, R. A. et al. Preventive effects of polyphenol E on urinary bladder and mammary cancers in rats and correlations with serum and urine levels of tea polyphenols. *Mol. Cancer Ther.* **6**, 2022–2028 (2007).
73. Puligundla, P., Mok, C., Ko, S. & Liang, J. & N. Recharla. Nanotechnological approaches to enhance the bioavailability and therapeutic efficacy of green tea polyphenols. *J. Funct. Foods*. **34**, 139–151 (2017).
74. Chanphai, P. & Tajmir-Riahi, H. A. Conjugation of tea catechins with Chitosan nanoparticles. *Food Hydrocoll.* **84**, 561–570 (2018).
75. Saleh, L., Ragab, E. A., Abdelhakim, H. K. & Mohamed, S. H. & Z. Zakaria. Evaluation of anticancer activities of Gallic acid and tartaric acid vectorized on iron oxide nanoparticles. *Drug Delivery Lett.* **10**, 123–132 (2020).
76. Jiang, Y., Zheng, T., Jin, W. & Shi, Y. Huang. Enhancing intestinal permeability of Theaflavin-3,3'-digallate by Chitosan-Caseinophosphopeptides nanocomplexes. *J. Agric. Food Chem.* **70**, 2029–2041 (2022).
77. Peng, H. & F. Shahidi. Oxidation and degradation of (epi)gallocatechin gallate (EGCG/GCG) and (epi)catechin gallate (ECG/CG) in alkali solution. *Food Chem.* **408**, 134815 (2022).

Author contributions

SAA involved in formal analysis, investigation, data curation, data validation, writing – original draft and writing – review & editing; NHS developed the conceptualization, methodology, provide software, resources, writing – review & editing, supervision, project administration and funding acquisition; AHI involved in investigation and writing – review & editing, NME involved in conceptualization, writing – review & editing, supervision and funding acquisition, LSP and AN involved in writing – review & editing and supervision.

Funding

The authors express their gratitude to the Ministry of Education, Malaysia, for providing project funding through

the Fundamental Research Grant Scheme (FRGS/1/2018/SKK10/UPM/02/5).

Declarations

Competing interests

The authors declare no competing interests.

Additional information

Correspondence and requests for materials should be addressed to N.H.S.

Reprints and permissions information is available at www.nature.com/reprints.

Publisher's note Springer Nature remains neutral with regard to jurisdictional claims in published maps and institutional affiliations.

Open Access This article is licensed under a Creative Commons Attribution-NonCommercial-NoDerivatives 4.0 International License, which permits any non-commercial use, sharing, distribution and reproduction in any medium or format, as long as you give appropriate credit to the original author(s) and the source, provide a link to the Creative Commons licence, and indicate if you modified the licensed material. You do not have permission under this licence to share adapted material derived from this article or parts of it. The images or other third party material in this article are included in the article's Creative Commons licence, unless indicated otherwise in a credit line to the material. If material is not included in the article's Creative Commons licence and your intended use is not permitted by statutory regulation or exceeds the permitted use, you will need to obtain permission directly from the copyright holder. To view a copy of this licence, visit <http://creativecommons.org/licenses/by-nc-nd/4.0/>.

© The Author(s) 2026